

# Accurate ab Initio Structure, Dissociation Energy, and Vibrational Spectroscopy of the $F^- - CH_4$ Anion Complex

Gábor Czako,\* Bastiaan J. Braams, and Joel M. Bowman

Cherry L. Emerson Center for Scientific Computation and Department of Chemistry, Emory University, Atlanta, Georgia 30322

Received: April 16, 2008; Revised Manuscript Received: May 26, 2008

Accurate equilibrium structure, dissociation energy, global potential energy surface (PES), dipole moment surface (DMS), and the infrared vibrational spectrum in the 0–3000  $cm^{-1}$  range of the  $F^- - CH_4$  anion complex have been obtained. The equilibrium electronic structure calculations employed second-order Møller–Plesset perturbation theory (MP2) and coupled-cluster (CC) method up to single, double, triple, and perturbative quadruple excitations using the aug-cc-p(C)VXZ [ $X = 2(D), 3(T), 4(Q),$  and  $5$ ] correlation-consistent basis sets. The best equilibrium geometry has been obtained at the all-electron CCSD(T)/aug-cc-pCVQZ level of theory. The dissociation energy has been determined based on basis set extrapolation techniques within the focal-point analysis (FPA) approach considering (a) electron correlation beyond the all-electron CCSD(T) level, (b) relativistic effects, (c) diagonal Born–Oppenheimer corrections (DBOC), and (d) variationally computed zero-point vibrational energies. The final  $D_e$  and  $D_0$  values are  $2398 \pm 12$  and  $2280 \pm 20$   $cm^{-1}$ , respectively. The global PES and DMS have been computed at the frozen-core CCSD(T)/aug-cc-pVTZ and MP2/aug-cc-pVTZ levels of theory, respectively. Variational vibrational calculations have been performed for  $CH_4$  and  $F^- - CH_4$  employing the vibrational configuration interaction (VCI) method as implemented in Multimode.

## 1. Introduction

As solvation and proton transfer play important roles in chemistry there have been many experimental and theoretical studies of ion–molecule complexes.<sup>1–8</sup> In particular, complexes and clusters composed of a halide anion and one or more second-row hydride molecules, e.g.,  $CH_4$ ,<sup>1–4</sup>  $NH_3$ ,<sup>5</sup>  $H_2O$ ,<sup>6,7</sup> and  $HF$ ,<sup>8</sup> have been examined employing infrared spectroscopy as well as ab initio methods. These molecules bind the halide anion by hydrogen bonds; in particular, the dimer complexes have a single hydrogen bond structure.

The  $X^- - CH_4$  anions, where X is a halogen, are being used as precursors in the novel photodetachment spectra to probe details of the reaction dynamics of the neutral systems,<sup>9</sup> and this adds to our motivation to study these anions. The present study focuses on the  $F^- - CH_4$  anion, which seems to be the most challenging halide–methane dimer complex, because the  $F^-$  anion perturbs strongly the electronic structure of the  $CH_4$  unit resulting in a large red-shift of the H-bonded CH stretching vibration ( $\nu_{hb}$ ). The measured  $\nu_{hb}$  frequency is 2535  $cm^{-1}$ , whereas the corresponding stretching fundamental of the free  $CH_4$  molecule is 2917  $cm^{-1}$ . The traditional harmonic frequency analysis fails to work since it overestimates the experimental value of the  $\nu_{hb}$  stretching mode. In 2004 Loh et al.<sup>2</sup> employed a local mode approximation for the H-bonded CH stretching, and they computed the  $\nu_{hb}$  frequency using a one-dimensional potential energy curve obtained at frozen-core MP2/aug-cc-pVTZ level of theory. In 2006 the same group performed vibrational self-consistent field (VSCF) calculations with second-order perturbation theory (PT2) corrections employing the frozen-core MP2/6-311++G(2df, 2p) level for the electronic structure calculations.<sup>3</sup> Even the scaled harmonic frequency

(2645  $cm^{-1}$ )<sup>3</sup> still overestimated the measured  $\nu_{hb}$  value, whereas the VSCF-PT2 result (2494  $cm^{-1}$ )<sup>3</sup> was below the experimental level.

In this paper we present highly accurate ab initio results for the equilibrium structure and for the dissociation energy ( $D_e$  and  $D_0$  values) of the  $F^- - CH_4$  anion complex. The previous studies<sup>2,3</sup> employed the MP2 method with triple- $\zeta$  basis functions correlating only the valance electrons. In our work the so-called focal-point analysis (FPA) approach<sup>10,11</sup> has been used to compute a benchmark  $D_e$  value. FPA utilizes electron correlation methods beyond the “gold standard” CCSD(T) level; in this study computations are performed up to the CCSDT(Q) level of theory, while the energies obtained at different basis sets are extrapolated in order to achieve the complete basis set (CBS) limit. In our calculations all the electrons are correlated, and the relativistic and non-Born–Oppenheimer effects have also been considered. Furthermore, we present a global potential energy surface (PES) and a dipole moment surface (DMS) for the  $F^- - CH_4$  anion computed at the frozen-core CCSD(T)/aug-cc-pVTZ and MP2/aug-cc-pVTZ levels of theory, respectively. Finally, employing the newly developed PES and DMS variational vibrational calculations are performed in full (12) dimensions in order to obtain converged vibrational energy levels and intensities for the  $F^- - CH_4$  system.

## 2. Computational Methods

The electronic structure calculations employed the augmented correlation-consistent polarized (core)/valance X zeta, aug-cc-p(C)VXZ [ $X = 2(D), 3(T), 4(Q),$  and  $5$ ],<sup>12</sup> basis sets. The use of the aug-cc-pCVXZ basis for a species containing hydrogen atoms means that the corresponding aug-cc-pVXZ basis was employed for the H atoms. Reference electronic wave functions were determined by the single-configuration restricted Hartree–

\* Corresponding author. E-mail: czako@chem.elte.hu.

Fock (RHF) method.<sup>13</sup> Both the closed-shell second-order Møller–Plesset perturbation theory (MP2)<sup>14</sup> and the coupled-cluster (CC)<sup>15</sup> methods including all single and double (CCSD) and triple (CCSDT) excitations as well as the CCSD(T)<sup>16</sup> and CCSDT(Q)<sup>17</sup> methods including perturbative triple (T) and quadruple (Q) terms were employed for treating electron correlation. In this study FC denotes the use of the frozen-core approach for the electron correlation calculations, whereas AE means computations when all the electrons are correlated.

Geometry optimizations at MP2 and CCSD(T) levels were performed by the program package MOLPRO<sup>18</sup> using analytical and numerical gradients, respectively. All the single-point energies for the FPA approach up to the all-electron CCSD(T) level as well as the PES and DMS at the FC-CCSD(T)/aug-cc-pVTZ and FC-MP2/aug-cc-pVTZ levels, respectively, were also computed by MOLPRO. The MRCC program<sup>19,20</sup> was employed for the all-electron CCSDT and CCSDT(Q) computations. The diagonal Born–Oppenheimer corrections (DBOC)<sup>21</sup> were determined by the program package ACESII.<sup>22</sup> The relativistic corrections were taken into account by using the Douglas–Kroll<sup>23</sup> relativistic one-electron integrals as implemented in MOLPRO.

The variational vibrational calculations were performed by the program package Multimode (MM)<sup>24,25</sup> using the vibrational configuration interaction (VCI) method. MM employs the exact kinetic energy operator of the Watson Hamiltonian<sup>26</sup> for nonlinear molecules. For the potential, the  $\pi\mu\pi$  terms (specifically the inverse of the effective moment of inertia), and the so-called “Watson term” in the kinetic energy operator,  $n$ -mode representations ( $n$ MRs)<sup>27,28</sup> are used. The value of  $n$  for these terms can be varied independently in MM and is typically between 3 and 5 and varied to check the convergence of vibrational energies. In the current version of MM the maximum value of  $n$  is 6(4) for the PES (inverse of the effective moment of inertia). It is important to note that the PES can be given in arbitrary curvilinear coordinates and MM, which employs rectilinear normal coordinates, calculates automatically the  $n$ -mode representation of the PES. The primitive basis functions are the eigenfunctions of the harmonic oscillator Hamiltonian, whereas the one-dimensional integrals are calculated using Gauss–Hermite quadrature weights and points. The multidimensional VCI basis functions are product of one-dimensional contracted functions. However, this VCI basis is not a direct product, since, in the current version of MM, only 5-mode excitations are simultaneously allowed. In our notation all  $i$ -mode, where  $i = 1-5$ , excitations are allowed to a maximum of  $N_i$  quanta in each mode. Furthermore, an upper limit of the sum of the quanta is set to  $M_i$  for the corresponding  $i$ -mode basis functions. In this paper let us denote a basis set as  $[N_{1M_1}, \dots, N_{i_{\max}M_{i_{\max}}}]$ , where the maximum number of the simultaneously excited modes is  $i_{\max}$ . For example, if no restriction is used for the sum of the quanta, i.e.,  $M_i = iN_i$ , the number of the functions in a  $D$ -dimensional basis can be obtained as

$$\sum_{i=0}^{i_{\max}} (N_i)^i \binom{D}{i} \quad (1)$$

In practical applications an  $M_i = N_i$  restriction is used. This truncation scheme keeps the size of the VCI matrix at modest levels, e.g., less than 30 000, even if 12 or more vibrational degrees of freedom are considered.

The integrals required for the finite basis representation (FBR) of the Hamiltonian are calculated using potential-optimized grid points. The  $n$ -mode representation of the PES ensures that only  $n$ -dimensional integrals have to be computed numerically, and

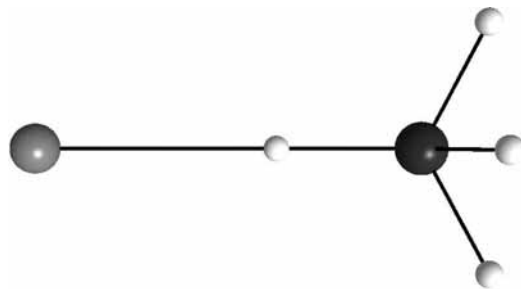


Figure 1. Equilibrium structure of the F<sup>-</sup>-CH<sub>4</sub> anion complex.

this is of course the major motivation for using the  $n$ MR of the potential (and also the inverse of the effective moment of inertia). As was also demonstrated in several previous studies,<sup>29</sup> even in the case of the 12-dimensional problem of the present work, the 4MR gives vibrational energy levels within about 1 cm<sup>-1</sup> corresponding to the given PES (as shown in detail in section 5).

In this study VCI calculations were performed employing  $n$ MRs up to  $n = 5$  and  $n = 4$  for the PES and the effective moment of inertia tensor, respectively. All the MM calculations were performed using 19 primitive functions and 28 Gauss–Hermite quadrature points for each mode. It was checked that an increase in the number of primitive functions and grid points does not result in significant changes, i.e., more than 1 cm<sup>-1</sup>, in the final results. MM employs  $N_i + 1$  contracted basis functions for each mode, while the number of the potential-optimized grid points is set to  $N_i + 1 + (28 - 19) = N_i + 10$  (increased by 1 if  $N_i + 10$  is odd).

### 3. Highly Accurate Equilibrium Structure and Dissociation Energy

**3.1. Equilibrium Structure.** As some previous studies reported,<sup>2,30,32</sup> the F<sup>-</sup>-CH<sub>4</sub> anion has a linear H-bonded C<sub>3v</sub> equilibrium structure as shown in Figure 1. As part of the present work optimized structural parameters have been computed at different levels of theory, and the results are summarized in Table 1. Our best estimates for the bond lengths  $r(\text{C}-\text{H})$ ,  $r(\text{C}-\text{H}_b)$ , and  $r(\text{F}-\text{H}_b)$ , where H<sub>b</sub> is the H-bonded hydrogen, are  $1.092 \pm 0.001$ ,  $1.109 \pm 0.001$ , and  $1.846 \pm 0.010$  Å, respectively, while the bond angle  $\alpha(\text{H}-\text{C}-\text{H}_b)$  is  $110.42 \pm 0.02^\circ$  obtained at the AE-CCSD(T)/aug-cc-pCVQZ level of theory. For comparison the CH distance in the free CH<sub>4</sub> is  $1.087 \pm 0.001$  Å at the same level of theory. The uncertainties are based on the results obtained at different levels of theory as given in Table 1. In the case of CH<sub>4</sub> the CH bond length agrees well with the best ab initio value ( $1.086$  Å)<sup>31</sup> which considers basis set extrapolation techniques as well as quadruple excitations. On the basis of these results it has been observed that the MP2 method underestimates the  $\alpha(\text{H}-\text{C}-\text{H}_b)$  by  $0.10^\circ$  and the CH and CH<sub>b</sub> distances by about  $0.004$  Å and overestimates the F<sup>-</sup>-H<sub>b</sub> separation by an averaged value of  $0.015$  Å. The effect of the core electron correlation results in a small decrease of about  $0.001$  Å in the bond lengths. The bond angle  $\alpha(\text{H}-\text{C}-\text{H}_b)$  decreases by  $0.02^\circ$  if all the electrons are correlated. In the case of the F<sup>-</sup>-CH<sub>4</sub> anion the previous studies employed B3LYP/6-31+G\*,<sup>32</sup> FC-MP2/aug-cc-pVTZ,<sup>2</sup> and FC-MP2/6-311++G(2df, 2p)<sup>3</sup> levels obtaining F<sup>-</sup>-H<sub>b</sub> separations of 1.88, 1.868, 1.840 Å, respectively. Finally, it is important to note that augmented basis functions have to be used in order to obtain reasonable structural parameters especially in the case of the F<sup>-</sup>-H<sub>b</sub> distance, since the AE-CCSD(T)  $r(\text{F}-\text{H}_b)$  values are 1.565, 1.648, and 1.716 Å employing cc-pCVDZ, cc-pCVTZ, and cc-pCVQZ basis sets,

**TABLE 1: Equilibrium Structures of CH<sub>4</sub> and the F<sup>-</sup>-CH<sub>4</sub> Anion Complex at Different Levels of Theory<sup>a</sup>**

methods <sup>b</sup>	CH <sub>4</sub> ( <i>T<sub>d</sub></i> )		F <sup>-</sup> -CH <sub>4</sub> ( <i>C<sub>3v</sub></i> )		
	<i>r</i> (C-H)	<i>r</i> (C-H)	<i>r</i> (C-H <sub>b</sub> )	<i>r</i> (F-H <sub>b</sub> )	α(H-C-H <sub>b</sub> )
FC-MP2/aug-cc-pVDZ	1.098	1.103	1.119	1.873	110.51
AE-MP2/aug-cc-pCVDZ	1.097	1.102	1.118	1.868	110.50
FC-MP2/aug-cc-pVTZ	1.086	1.091	1.109	1.868	110.34
AE-MP2/aug-cc-pCVTZ	1.085	1.089	1.107	1.871	110.33
FC-MP2/aug-cc-pVQZ	1.085	1.089	1.108	1.857	110.35
AE-MP2/aug-cc-pCVQZ	1.083	1.087	1.106	1.858	110.32
FC-CCSD(T)/aug-cc-pVDZ	1.103	1.108	1.123	1.854	110.61
FC-CCSD(T)/aug-cc-pCVDZ	1.102	1.108	1.122	1.853	110.60
AE-CCSD(T)/aug-cc-pCVDZ	1.101	1.107	1.122	1.850	110.60
FC-CCSD(T)/aug-cc-pVTZ	1.090	1.095	1.111	1.852	110.44
FC-CCSD(T)/aug-cc-pCVTZ	1.090	1.095	1.111	1.857	110.45
AE-CCSD(T)/aug-cc-pCVTZ	1.088	1.094	1.110	1.856	110.42
FC-CCSD(T)/aug-cc-pVQZ	1.088	1.094	1.110	1.844	110.44
FC-CCSD(T)/aug-cc-pCVQZ	1.088	1.094	1.110	1.846	110.44
AE-CCSD(T)/aug-cc-pCVQZ	1.087	1.092	1.109	1.846	110.42

<sup>a</sup> All the bond lengths (*r*) are in angstroms and the bond angle (α) is in degrees. H<sub>b</sub> denotes the H-bonded hydrogen atom. Since F<sup>-</sup>-CH<sub>4</sub> has a linear H-bonded *C<sub>3v</sub>* structure  $r(\text{C-F}) = r(\text{C-H}_b) + r(\text{F-H}_b)$ . <sup>b</sup> FC and AE denote frozen-core and all-electron computations, respectively.

**TABLE 2: Focal-Point Analysis of the All-Electron Nonrelativistic Born–Oppenheimer Dissociation Energy (*D<sub>e</sub>*, cm<sup>-1</sup>) of the F<sup>-</sup>-CH<sub>4</sub> Anion Complex<sup>a</sup>**

	<i>D<sub>e</sub></i> [RHF]	δ[MP2]	δ[CCSD]	δ[CCSD(T)]	δ[CCSDT]	δ[CCSDT(Q)]	<i>D<sub>e</sub></i>
aug-cc-pCVDZ	1587.1	+787.8	+17.8	+191.6	+10.6	-1.0	2594.1
aug-cc-pCVTZ	1474.6	+821.4	+10.8	+172.6	[+10.6]	[-1.0]	2489.0
aug-cc-pCVQZ	1474.9	+808.8	+3.4	+161.3	[+10.6]	[-1.0]	2458.0
aug-cc-pCV5Z	1467.9	+787.5	+1.7	[+161.3]	[+10.6]	[-1.0]	2428.1
CBS <sup>b</sup>	1466.7	+765.2	-0.1	+153.2	+10.6	-1.0	2394.6

<sup>a</sup> The results correspond to the structures optimized at the AE-CCSD(T)/aug-cc-pCVQZ level of theory. For the all-electron correlation methods the symbol δ denotes the increments in *D<sub>e</sub>* with respect to the preceding level of theory. Brackets signify assumed, nonextrapolated, increments from smaller basis set results. <sup>b</sup> The complete basis set (CBS) RHF energy and the MP2, CCSD, and CCSD(T) electron correlation energies were calculated using two-parameter extrapolation formulas given in eqs 2 and 3, respectively. Only the best two energies were included in the extrapolations.

respectively, whereas the corresponding results obtained with augmented basis sets are 1.850, 1.856, and 1.846 Å, in order.

**3.2. Dissociation Energy.** The dissociation energy corresponding to the F<sup>-</sup>-CH<sub>4</sub> → F<sup>-</sup> + CH<sub>4</sub> channel has been determined using the FPA approach, and the results are presented in Table 2. Single-point electron energy calculations have been performed for the three species, F<sup>-</sup>-CH<sub>4</sub>, CH<sub>4</sub>, and F<sup>-</sup>, using the AE-CCSD(T)/aug-cc-pCVQZ reference structures for F<sup>-</sup>-CH<sub>4</sub> and CH<sub>4</sub>. The aug-cc-pCVXZ basis sets have been employed, where *X* = D(2)–5 for the RHF, AE-MP2, and AE-CCSD calculations and *X* = D(2)–Q(4) for the AE-CCSD(T) method. Electron correlation energies have also been taken into account beyond the AE-CCSD(T) level by performing AE-CCSDT and AE-CCSDT(Q) calculations using the aug-cc-pCVDZ basis set.

The RHF energies have been extrapolated to determine the RHF CBS limit,  $E_{\text{CBS}}^{\text{RHF}}$ , employing a two-parameter formula<sup>33</sup>

$$E_X^{\text{RHF}} = E_{\text{CBS}}^{\text{RHF}} + a(X+1)e^{-9\sqrt{X}} \quad (2)$$

where  $E_X^{\text{RHF}}$  is the RHF energy obtained by the corresponding aug-cc-pCVXZ basis. The extrapolations have been performed for all the three individual species using the best two energies, i.e., *X* = Q(4) and 5. Since the RHF energies converge exponentially the difference between the RHF CBS limit of the *D<sub>e</sub>* value and the *D<sub>e</sub>* obtained at the RHF/aug-cc-pCV5Z level is only 1.2 cm<sup>-1</sup>.

The electron correlation energies,  $E_X$ , have been extrapolated using a two-parameter polynomial formula<sup>34</sup>

$$E_X = E_{\text{CBS}} + bX^{-3} \quad (3)$$

where  $E_{\text{CBS}}$  is the CBS limit of the correlation energy. In order to get the best estimates for the CBS limits the energies obtained by the largest two basis sets were included in the extrapolations, namely, *X* = Q(4) and 5 in the cases of the MP2 and CCSD levels and *X* = T(3) and Q(4) for the CCSD(T) level. The aug-cc-pCV5Z and CBS δ[MP2] increments deviate by 22.3 cm<sup>-1</sup> causing the largest uncertainty in the *D<sub>e</sub>* value. Interestingly the extrapolated δ[CCSD] increment with respect to the MP2 level is only -0.1 cm<sup>-1</sup>; thus, the *D<sub>e</sub>* values at the MP2 and CCSD levels are almost the same. As expected the convergence of the correlation energy increments is better for the higher excitations; thus, the extrapolated δ[CCSD(T)] increment is only 8.1 cm<sup>-1</sup> below the corresponding aug-cc-pCVQZ basis set result. The contribution of the electron correlation energies to the *D<sub>e</sub>* value is extremely large, since the CBS RHF *D<sub>e</sub>* value is only 1466.7 cm<sup>-1</sup>, whereas the effects of all the single and double, all the triple, and the perturbative quadruple excitations are +765.1, +163.8, and -1.0 cm<sup>-1</sup>, respectively. The effect of the neglected excitations beyond the perturbatively estimated quadruples is likely to be less than 1 cm<sup>-1</sup>. Our best estimate for the all-electron nonrelativistic BO *D<sub>e</sub>* value of the F<sup>-</sup>-CH<sub>4</sub> anion complex is 2395 ± 10 cm<sup>-1</sup>.

Relativistic electronic structure calculations have been performed using the Douglas–Kroll relativistic one-electron integrals. The relativistic effect on the value of *D<sub>e</sub>* has been found to be negligibly small, since it is +1.5 cm<sup>-1</sup> at the AE-CCSD(T)/aug-cc-pCVQZ level of theory. The DBOCs have also been



TABLE 3: Properties of the Global Potential Energy Surface (PES) of the F<sup>-</sup>-CH<sub>4</sub> Anion Complex

	global minimum (F <sup>-</sup> -CH <sub>4</sub> )			CH <sub>4</sub> + F <sup>-</sup> channel			CH <sub>3</sub> <sup>-</sup> + HF channel				
	PES <sup>a</sup>	opt. <sup>b</sup>	acc. <sup>c</sup>	PES <sup>a</sup>	opt. <sup>b</sup>	acc. <sup>c</sup>	PES <sup>a</sup>	opt. <sup>b</sup>	acc. <sup>c</sup>		
				Structures <sup>d</sup>							
<i>r</i> (C-H)	1.095	1.095	1.092	<i>r</i> (C-H)	1.090	1.090	1.087	<i>r</i> (C-H)	1.106	1.105	1.100
<i>r</i> (C-H <sub>b</sub> )	1.112	1.111	1.109					α(H-C-H)	109.11	108.73	109.31
<i>r</i> (F-H <sub>b</sub> )	1.846	1.852	1.846					<i>r</i> (H-F)	0.921	0.921	0.917
α(H-C-H <sub>b</sub> )	110.46	110.44	110.42								
				Relative Energies (cm <sup>-1</sup> )							
	0	0	0	2434	2523	2448 <sup>e</sup>	0	19 324	19 548	19 582	

<sup>a</sup> Results corresponding to the global fitted PES of F<sup>-</sup>-CH<sub>4</sub> based on FC-CCSD(T)/aug-cc-pVTZ energy points. <sup>b</sup> Results obtained by ab initio calculations at the FC-CCSD(T)/aug-cc-pVTZ level of theory. <sup>c</sup> Accurate results obtained at the AE-CCSD(T)/aug-cc-pCVQZ level of theory. <sup>d</sup> All the bond lengths (*r*) are in angstroms and the bond angles (α) are in degrees. H<sub>b</sub> denotes the H-bonded hydrogen atom. <sup>e</sup> The highly accurate value is 2398 cm<sup>-1</sup> (see section 3.2.).

computed at the RHF/aug-cc-pVTZ(aug-cc-pVDZ) level, and the correction to the *D<sub>e</sub>* value is only +2.1(1.9) cm<sup>-1</sup>. Thus, it is likely that the breakdown of the BO approach does not compromise the accuracy of the *D<sub>e</sub>* of the F<sup>-</sup>-CH<sub>4</sub> anion. If these two small corrections have been taken into account, we arrive to our best relativistic non-BO *D<sub>e</sub>* value of 2398 ± 12 cm<sup>-1</sup>.

Finally, utilizing the variationally computed zero-point vibrational energy (ZPVE) values of CH<sub>4</sub> and F<sup>-</sup>-CH<sub>4</sub>, i.e., 9677 and 9795 cm<sup>-1</sup> (see section 5), respectively, a ZPVE correction of -118 cm<sup>-1</sup> can be employed to calculate the *D<sub>0</sub>* value of the F<sup>-</sup>-CH<sub>4</sub> anion complex. Since the ZPVE values of both species have been computed using the same PES the uncertainty of the ZPVE correction is likely to be smaller than the uncertainties of the individual ZPVEs. Our final estimate for the *D<sub>0</sub>* value of the F<sup>-</sup>-CH<sub>4</sub> anion complex is 2280 ± 20 cm<sup>-1</sup>.

In the early work of Novoa et al.<sup>30</sup> a computed *D<sub>e</sub>* value of 2100 ± 200 cm<sup>-1</sup> (originally reported as 6.1 ± 0.5 kcal mol<sup>-1</sup>) was published. In 2006 a theoretical study<sup>3</sup> obtained a *D<sub>0</sub>* value of 2420 cm<sup>-1</sup> employing the FC-MP2/6-311++G(2df, 2p) level and harmonic ZPVE correction. Hiraoka and co-workers<sup>32</sup> measured an association enthalpy of 2340 ± 70 cm<sup>-1</sup> for F<sup>-</sup>-CH<sub>4</sub> with a pulsed electron beam high-pressure mass spectrometer. The computed *D<sub>0</sub>* value reported in the present work (2280 ± 20 cm<sup>-1</sup>) is just within the given error bar of the experimental result, but we believe our computed value has much better accuracy and lower uncertainty than the measured and previous theoretical binding energies.

#### 4. Global Potential Energy and Dipole Moment Surfaces

Electronic energies for the global PES and dipole moments for the DMS of the F<sup>-</sup>-CH<sub>4</sub> anion complex were computed at the FC-CCSD(T)/aug-cc-pVTZ and the FC-MP2/aug-cc-pVTZ levels of theory, respectively. Ab initio calculations for the complex region were combined with calculations for two possible fragment channels: CH<sub>4</sub> + F<sup>-</sup> and CH<sub>3</sub><sup>-</sup> + HF. The fitted PES is based on 6546 ab initio energies in the complex region and 3000 energies in each of the two relevant fragment channels. The fitted DMS is based on 7586 ab initio dipole moments in the complex region and again 3000 in each of the two fragment channels. As described previously<sup>35,36</sup> in applications to molecules with as many as nine atoms the PES is represented by a polynomial expansion in Morse-like variables of the internuclear distances,  $y(i, j) = \exp(-r(i, j)/a)$  where  $a = 2.0$  bohr and using a compact polynomial basis that is explicitly invariant under permutations of like atoms. We

included all terms up to total degree 6, and the associated vector space of invariant polynomials is of dimension 3250. In addition, three free coefficients were used to represent short-term repulsion for each of the four possible pairs (HH, HC, HF, and CF), giving a total of 3262 free coefficients.

A weighted least-squares fit was constructed in which a configuration at energy *E* relative to the global minimum has weight  $E_0/(E + E_0)$  where  $E_0 = 0.1$  hartree. The rms fitting error is 42 cm<sup>-1</sup> over the subset of configurations that have energy at most 22 000 cm<sup>-1</sup> above the global minimum; it is 1200 cm<sup>-1</sup> for the subset of configurations that have energy in the range of 22 000–44 000 cm<sup>-1</sup> relative to the global minimum and 1400 cm<sup>-1</sup> for the subset of configurations in the range of 44 000–110 000 cm<sup>-1</sup> above the global minimum of the PES.

Properties of the global PES are given in Table 3 including the structures corresponding to the global minimum and the two possible fragment channels. The relative energies with respect to the global minimum are given for both fragment channels. Relevant results are also shown in Table 3 based on geometry optimizations performed by MOLPRO employing the same FC-CCSD(T)/aug-cc-pVTZ level of theory as this level has been employed for the determination of the energy points for the fitting procedure. For comparison accurate results are also presented computed at the AE-CCSD(T)/aug-cc-pCVQZ level of theory. The FC-CCSD(T)/aug-cc-pVTZ dissociation energies for the channels CH<sub>4</sub> + F<sup>-</sup> and CH<sub>3</sub><sup>-</sup> + HF are 2434(2523) and 19 324(19 548) cm<sup>-1</sup> corresponding to the fitted global PES(individually optimized structures), respectively. The discrepancies between the dissociation energies obtained via different ways are in agreement with the given rms errors of the fitting method. In the case of the CH<sub>3</sub><sup>-</sup> + HF fragment channel, the *C<sub>3v</sub>* point-group symmetry of the CH<sub>3</sub><sup>-</sup> anion has been obtained within the expected numerical precision and the CH and HF bond lengths corresponding to the PES are accurate within the required precision of the FC-CCSD(T)/aug-cc-pVTZ level of theory.

The DMS is represented via effective charges at the positions of the nuclei. These fitted effective charges are made to transform as a covariant under permutation of like nuclei. Again, an expansion in Morse-like variables of the internuclear distances is employed, plus six free coefficients for each possible pair of unlike atoms and three free coefficients for the HH pair. The total number of free coefficients in the dipole moment expansion is 1560. The rms error for the dipole fit is 0.064 au for the subset of configurations having energy in the range of

**TABLE 4: Zero-Point Vibrational Energies, All the Fundamentals, and Selected Overtone and Combination Levels (all in  $\text{cm}^{-1}$ ) as Well as Intensities ( $I$ ,  $\text{km mol}^{-1}$ ) for  $\text{CH}_4$  and  $\text{F}^- - \text{CH}_4$** 

	$\text{CH}_4$				$\text{F}^- - \text{CH}_4$			
	exptl <sup>a</sup>		VCI <sup>c</sup>		exptl <sup>a</sup>		VCI <sup>c</sup>	
	$\nu$	harm. <sup>b</sup> $\omega$	$\nu$	$I$	$\nu$	harm. <sup>b</sup> $\omega$	$\nu$	$I$
$\nu_0(a_1)$		9824	9677		$\nu_0(a_1)$	9967	9795	
					$\nu_5(a_1)$	200	201	79
					$\nu_6(e)$	276	300	1
					$2\nu_5(a_1)$	400	391	5
$\nu_4(t_2)$	1311	1357	1315	27	$\nu_4(a_1)$	1296	1244	0
					$\nu_4(e)$	1395	1353	4
$\nu_2(e)$	1533	1565	1532	0	$\nu_2(e)$	1570	1532	1
					$[\nu_6(e) + \nu_4(e)](a_1)$	1671	1649	15
					$[\nu_6(e) + \nu_2(e)](a_1)$	1846	1829	25
$2\nu_4(a_1)$	2587	2714	2590	2	$2\nu_4(a_1)$	2592	2464	16
$2\nu_4(t_2)$	2614	2714	2621	0	$\nu_4(a_1) + \nu_4(e)$	2691	2599	0
$2\nu_4(e)$	2625	2714	2631	0	$[2\nu_4(e)](e)$	2790	2697	2
					$[2\nu_4(e)](a_1)$	2745 <sup>d</sup>	2790	2705
$\nu_1(a_1)$	2917	3018	2906	4	$\nu_{\text{hb}}(a_1)$	2535	2782	2519
					$\nu_5(a_1) + \nu_{\text{hb}}(a_1)$		2982	2755
$[\nu_2(e) + \nu_4(t_2)](t_2)$	2830	2922	2832	7	$\nu_2(e) + \nu_4(a_1)$		2866	2773
$[\nu_2(e) + \nu_4(t_2)](t_1)$	2846	2922	2849	0	$[\nu_2(e) + \nu_4(e)](e)$		2965	2893
					$[\nu_2(e) + \nu_4(e)](a_1)$		2965	2894
$\nu_3(t_2)$	3020	3143	3006	128	$\nu_3(a_1)^e$		3024	2859 <sup>e</sup>
					$\nu_3(e)$	2956	3074	2937
								215

<sup>a</sup> Experimental levels for  $\text{CH}_4$  and  $\text{F}^- - \text{CH}_4$  were taken from refs 41 and 3, respectively. <sup>b</sup> Harmonic frequencies corresponding to the (constrained) fitted PES of ( $\text{CH}_4$ )  $\text{F}^- - \text{CH}_4$  (see details in the text). Harmonic frequencies of the overtones and combination levels are taken as the sum of the corresponding fundamentals. <sup>c</sup> Vibrational configuration interaction (VCI) energies and wave functions were computed with 4MR using the [7<sub>7</sub>6<sub>7</sub>5<sub>7</sub>3<sub>6</sub>2<sub>6</sub>] basis of 6406 and 21 348 functions for  $\text{CH}_4$  and  $\text{F}^- - \text{CH}_4$ , respectively. <sup>d</sup> We assume that the observed band at 2745  $\text{cm}^{-1}$  is not the  $[2\nu_4(e)](a_1)$  (see section 5.2 for more details). <sup>e</sup> This level has a VCI coefficient of 0.66, and another state at 2912  $\text{cm}^{-1}$  with 1  $\text{km mol}^{-1}$  intensity has also a significant VCI coefficient of 0.49 corresponding to the same fundamental mode.

0–0.1  $E_h$  relative to the global minimum of the PES, increasing to 0.21 au for configurations having energy in the range of 0.1–0.2  $E_h$  and to 0.44 au for configurations having energy in the range of 0.2–0.5  $E_h$ .

## 5. Variational Vibrational Calculations

**5.1.  $\text{CH}_4$  Limit.** As a test of the newly developed global surfaces variational vibrational calculations have been performed for  $\text{CH}_4$  using the PES of the  $\text{F}^- - \text{CH}_4$  anion. In order to use the PES for  $\text{CH}_4$  the  $\text{F}^- - \text{C}$  separation was set to a fixed value of 100 bohr. The nine-dimensional VCI calculations have been performed using the reference geometry corresponding to the global minimum of the constrained PES. The  $T_d$  point-group symmetry of the equilibrium structure of  $\text{CH}_4$  has been obtained within numerical precision, and the CH bond length was 1.090 Å. This value has been found identical with the parameter obtained by MOLPRO using the same FC-CCSD(T)/aug-cc-pVTZ level of theory. The reduced dimensionality DMS for  $\text{CH}_4$ ,  $\mu_{\text{CH}_4}(\mathbf{x}_{\text{CH}_4})$ , where  $\mathbf{x}_{\text{CH}_4}$  contains the  $5 \times 3$  Cartesian coordinates of  $\text{CH}_4$ , was obtained from the DMS of  $\text{F}^- - \text{CH}_4$ ,  $\mu_{\text{F}^- - \text{CH}_4}$ , as

$$\mu_{\text{CH}_4}(\mathbf{x}_{\text{CH}_4}) = \mu_{\text{F}^- - \text{CH}_4}(\mathbf{x}_{\text{CH}_4}, \mathbf{x}_{\text{F}^-}) + \mathbf{x}_{\text{F}^-} \quad (4)$$

In eq 4  $\mathbf{x}_{\text{F}^-} = (x_C + 100, y_C, z_C)$  bohr, where  $x_C$ ,  $y_C$ , and  $z_C$  are the Cartesian coordinates of the C atom; thus, the  $\text{F}^- - \text{C}$  separation was fixed at 100 bohr, and the dipole contribution of  $\text{F}^- (-\mathbf{x}_{\text{F}^-})$  was subtracted from the constrained DMS of the  $\text{F}^- - \text{CH}_4$  anion. Selected vibrational levels and intensities are given in Table 4. The harmonic frequencies correspond to the PES, and the differences between the given values and the frequencies obtained by finite difference formulas based on highly accurate energy points computed at the same level of theory are less than 10  $\text{cm}^{-1}$ . These deviations are due to the

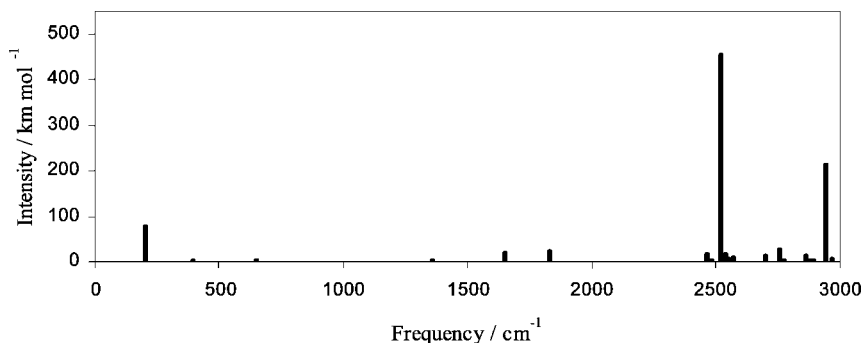
fitting error of the PES. The variationally computed vibrational energies of  $\text{CH}_4$  are in good agreement with the experimentally observed levels and the previous theoretical values.<sup>29,37–40</sup> The deviation between the computed and observed fundamentals is less than 8  $\text{cm}^{-1}$  on the average. This indicates that an error bar of around 10–15  $\text{cm}^{-1}$  can be expected in the case of the  $\text{F}^- - \text{CH}_4$  anion, which discrepancy may correspond to the inaccuracy of the global PES.

**5.2.  $\text{F}^- - \text{CH}_4$  Anion Complex.** The vibrational energy levels and wave functions for the  $\text{F}^- - \text{CH}_4$  anion have been obtained by VCI calculations in 12 dimensions. Employing the variationally computed vibrational wave functions and the DMS infrared intensities have been determined at 0 K. Due to the fact that the  $\text{F}^- - \text{CH}_4$  anion is a floppy system several computations have been performed in order to check the convergence of the MM calculations. In the VCI calculations no symmetry has been assumed; thus, the degenerate vibrational states should be obtained numerically. In Table 5 VCI results for  $\text{F}^- - \text{CH}_4$  have been summarized obtained by using different  $n$ MRs and basis sets. First, MM calculations were performed using 2(2), 3(3), 4(4), and 5(4) MRs for the PES (effective moment of inertia tensor) employing the same [7<sub>7</sub>5<sub>8</sub>3<sub>6</sub>2<sub>5</sub>1<sub>5</sub>] basis of 8544 functions. The differences between the frequencies obtained with  $n$ MR and  $(n-1)$ MR (denoted as  $\delta[n\text{MR}]$ ) as well as the numerical split errors for the degenerate states are given. These energy differences show much faster convergence than the corresponding absolute values; thus, they can be computed using a modest basis size. The differences between the frequencies obtained with 2MR and 3MR can be larger than 10  $\text{cm}^{-1}$ . Fortunately, these  $\delta[n\text{MR}]$  deviations decrease greatly employing 4MR and 5MR. In the case of the  $\nu_{\text{hb}}$  value the  $\delta[3\text{MR}]$ ,  $\delta[4\text{MR}]$ , and  $\delta[5\text{MR}]$  frequency increments are +34.7, -2.8, +1.1  $\text{cm}^{-1}$ , respectively. The  $\delta[5\text{MR}]$  values given in Table 5 show that

**TABLE 5: Convergence of the Zero-Point Vibrational Energy and the Fundamental Frequencies, in cm<sup>-1</sup>, of F<sup>-</sup>-CH<sub>4</sub><sup>a</sup>**

<i>n</i> MR	2MR	δ[3MR]	δ[4MR]	δ[5MR]	4MR	4MR	4MR	4MR	4MR
matrix size	8544	8544	8544	8544	1820	6188	17640	21348	21348
basis	[775 <sub>8</sub> 3 <sub>6</sub> 2 <sub>5</sub> 1 <sub>5</sub> ]	[775 <sub>8</sub> 3 <sub>6</sub> 2 <sub>5</sub> 1 <sub>5</sub> ]	[775 <sub>8</sub> 3 <sub>6</sub> 2 <sub>5</sub> 1 <sub>5</sub> ]	[775 <sub>8</sub> 3 <sub>6</sub> 2 <sub>5</sub> 1 <sub>5</sub> ]	[4 <sub>4</sub> 3 <sub>4</sub> 2 <sub>4</sub> 1 <sub>4</sub> ]	δ[5 <sub>4</sub> 5 <sub>3</sub> 5 <sub>2</sub> 5 <sub>1</sub> 5 <sub>1</sub> ]	δ[6 <sub>6</sub> 5 <sub>6</sub> 4 <sub>6</sub> 3 <sub>6</sub> 2 <sub>6</sub> ]	δ[7 <sub>7</sub> 6 <sub>7</sub> 5 <sub>7</sub> 3 <sub>6</sub> 2 <sub>6</sub> ]	[7 <sub>7</sub> 6 <sub>7</sub> 5 <sub>7</sub> 3 <sub>6</sub> 2 <sub>6</sub> ]
<i>v</i> <sub>0</sub> ( <i>a</i> <sub>1</sub> )	9813.9	-13.6	-0.3	+1.1	9807.8	-4.9	-6.4	-1.8	9794.7
<i>v</i> <sub>3</sub> ( <i>a</i> <sub>1</sub> )	201.0	-0.1	+0.2	-0.1	211.4	-12.0	+1.3	+0.4	201.1
<i>v</i> <sub>b</sub> ( <i>e</i> )	320.6(11.2)	-12.4(3.1)	-3.1(0.4)	+1.4(0.2)	347.3	-33.2	-8.4	-5.8	299.9
<i>v</i> <sub>4</sub> ( <i>a</i> <sub>1</sub> )	1269.7	-24.1	-0.1	+2.0	1267.9	-23.0	-1.2	+0.1	1243.9
<i>v</i> <sub>4</sub> ( <i>e</i> )	1357.9(4.0)	-8.3(0.9)	+4.2(0.4)	+0.6(0.2)	1369.8	-16.2	-0.7	-0.3	1352.7
<i>v</i> <sub>2</sub> ( <i>e</i> )	1547.0(0.9)	-18.9(3.7)	+6.1(0.4)	+1.2(0.3)	1549.3	-15.3	-1.3	-0.4	1532.4
<i>v</i> <sub>hb</sub> ( <i>a</i> <sub>1</sub> )	2493.5	+34.7	-2.8	+1.1	2557.6	-28.5	-7.5	-2.5	2519.2
<i>v</i> <sub>3</sub> ( <i>a</i> <sub>1</sub> ) <sup>b</sup>	2774.0	+86.2	+6.0	+1.7	2905.2	-40.1	-5.9	-0.6	2858.7
<i>v</i> <sub>3</sub> ( <i>e</i> )	2867.7(67.1)	+77.8(9.1)	-2.8(0.1)	+1.1(1.5)	2955.4	-13.7	-3.2	-1.1	2937.3

<sup>a</sup> The symbol  $\delta$  denotes the increments in the vibrational energies with respect to the preceding level of theory. The calculations employed  $C_1$  symmetry; thus, the degenerate levels were obtained twice. In this table the average values are shown while the differences between the numerically split levels are given in parentheses. <sup>b</sup> See footnote e of Table 4.

**Figure 2.** Computed vibrational spectrum of F<sup>-</sup>-CH<sub>4</sub> in the 0–3000 cm<sup>-1</sup> range.

the vibrational energy levels corresponding to 4MR and 5MR agree within 1 or 2 cm<sup>-1</sup>. The degeneracy of most of the *e* symmetry modes cannot be obtained within a few wavenumbers using the 2MR; however, in the case of the 4MR the degenerate levels are within 1 cm<sup>-1</sup> even if  $C_1$  point-group symmetry is used in the calculations. On the basis of this first part of the convergence test one can state that the 4MR results are converged within the requested precision of the present study, and it is not worth employing the computationally much more expensive 5MR with a more complete basis set. Therefore, VCI calculations have been performed using 4MR employing different basis sets. The basis set convergence study started with the modest [4<sub>4</sub>3<sub>4</sub>2<sub>4</sub>1<sub>4</sub>] basis, and the average  $\delta$ [5<sub>4</sub>5<sub>3</sub>5<sub>2</sub>5<sub>1</sub>5<sub>1</sub>],  $\delta$ [6<sub>6</sub>5<sub>6</sub>4<sub>6</sub>3<sub>6</sub>2<sub>6</sub>], and  $\delta$ [7<sub>7</sub>6<sub>7</sub>5<sub>7</sub>3<sub>6</sub>2<sub>6</sub>] absolute increments with respect to the preceding basis are 20.8, 4.0, and 1.4 cm<sup>-1</sup>, respectively. The final results were computed using the [7<sub>7</sub>6<sub>7</sub>5<sub>7</sub>3<sub>6</sub>2<sub>6</sub>] basis of 21348 functions.

Selected vibrational energy levels, including all the fundamentals, of F<sup>-</sup>-CH<sub>4</sub> are given in Table 4. It is useful to note that the harmonic frequencies correspond to the fitted PES; thus, they differ by a few wavenumbers from the results obtained by standard program packages using the same level of theory. The highest anharmonicities can be observed in the stretching fundamentals, *v*<sub>hb</sub>(*a*<sub>1</sub>), *v*<sub>3</sub>(*a*<sub>1</sub>), and *v*<sub>3</sub>(*e*), especially in the case of the *v*<sub>hb</sub> frequency, which corresponds to the CH stretch of the H-bond. The harmonic  $\omega_{hb}$  is 2782 cm<sup>-1</sup>, whereas the measured value is only 2535 cm<sup>-1</sup> (with a head at 2525 cm<sup>-1</sup>).<sup>3</sup> Our variational estimate for this mode is 2519 cm<sup>-1</sup>, which agrees well with the experimental frequency. All the stretching fundamentals are red-shifted relative to the corresponding frequencies of CH<sub>4</sub>. In the case of the F<sup>-</sup>-CH<sub>4</sub> anion complex there are two low-lying fundamentals, namely, *v*<sub>s</sub>(*a*<sub>1</sub>) at 201 cm<sup>-1</sup> and the degenerate *v*<sub>b</sub>(*e*) at 300 cm<sup>-1</sup>; these modes

correspond to the intermolecular stretching and bending vibrations, respectively. Interestingly the *v*<sub>s</sub>(*a*<sub>1</sub>) fundamental shows only a little anharmonicity, since the harmonic and VCI values agree within 1 cm<sup>-1</sup>.

The computed vibrational spectrum of the F<sup>-</sup>-CH<sub>4</sub> anion complex is shown in Figure 2 while the relevant intensity data are given in Table 4. The *v*<sub>hb</sub> fundamental has the highest intensity (456 km mol<sup>-1</sup>) in the 0–3000 cm<sup>-1</sup> range. The intensity of the degenerate *v*<sub>3</sub>(*e*) stretching mode is 215 km mol<sup>-1</sup>, whereas the other stretching level *v*<sub>3</sub>(*a*<sub>1</sub>) computed at 2859 cm<sup>-1</sup> has a lower intensity of 15 km mol<sup>-1</sup>. It is important to note that the VCI coefficient corresponding to the *v*<sub>3</sub>(*a*<sub>1</sub>) fundamental is only 0.66 in the case of the level at 2859 cm<sup>-1</sup>, whereas another state at 2912 cm<sup>-1</sup> with a very low intensity of 1 km mol<sup>-1</sup> has also a significant VCI coefficient of 0.49 corresponding to the same fundamental. Among the low-lying frequencies the *v*<sub>s</sub>(*a*<sub>1</sub>) state, which is the first peak in the spectrum, has a relatively large intensity, 79 km mol<sup>-1</sup>. The overtone of this fundamental has also been computed at 391 cm<sup>-1</sup>. This 2*v*<sub>s</sub>(*a*<sub>1</sub>) state has the second largest intensity (5 km mol<sup>-1</sup>) among the low-lying states, i.e., in the 0–1000 cm<sup>-1</sup> range. To the best of our knowledge all the previous measurements were reported in the CH stretching region; thus, the *v*<sub>s</sub>(*a*<sub>1</sub>) fundamental and its overtone have not been observed yet.

In 2006 Loh et al.<sup>3</sup> published a measured infrared spectrum for F<sup>-</sup>-CH<sub>4</sub> in the CH stretching region. The agreement between the two most intensive computed and measured states is good, since the computed(measured) *v*<sub>hb</sub>(*a*<sub>1</sub>) and *v*<sub>3</sub>(*e*) frequencies are 2519(2535) and 2937(2956) cm<sup>-1</sup>, respectively. There is a weak observed band at 2745 cm<sup>-1</sup>, with 0.07 intensity relative to *v*<sub>hb</sub>(*a*<sub>1</sub>), which was assigned to the *a*<sub>1</sub> component of 2*v*<sub>4</sub>(*e*). In 2002 the same authors predicted that this peak could be the combination of the *v*<sub>hb</sub>(*a*<sub>1</sub>) and the *v*<sub>s</sub>(*a*<sub>1</sub>) or *v*<sub>b</sub>(*e*) modes.<sup>1</sup>



The computations support the older assignment, since the computed  $\nu_s(a_1) + \nu_{hb}(a_1)$  combination level is at  $2755\text{ cm}^{-1}$  with an intensity of  $26\text{ km mol}^{-1}$ ; thus, the relative intensity is 0.06, which is similar to the observed value. It is important to note that the VCI coefficients for this state are 0.64 and 0.34 corresponding to the  $\nu_s(a_1) + \nu_{hb}(a_1)$  combination and the  $\nu_{hb}(a_1)$  fundamental, respectively. The  $a_1$  component of  $2\nu_4(e)$  has been computed at  $2705$  with  $(0.004) 2\text{ km mol}^{-1}$  (relative) intensity; therefore, we conclude that the observed band at  $2745$  is not the  $[2\nu_4(e)](a_1)$ .

## 6. Conclusions

Accurate equilibrium structure of the  $F^-CH_4$  anion complex,  $[r(C-H), r(C-H_b), r(F-H_b)] = (1.092 \pm 0.001, 1.109 \pm 0.001, 1.846 \pm 0.010)\text{ \AA}$  and  $\alpha(H-C-H_b) = 110.42 \pm 0.02^\circ$ , was obtained at the AE-CCSD(T)/aug-cc-pCVQZ level of theory. The MP2 method underestimates the  $\alpha(H-C-H_b)$  by  $0.10^\circ$  and the CH and  $CH_b$  distances by about  $0.004\text{ \AA}$  and overestimates the  $F^-H_b$  separation by about  $0.015\text{ \AA}$ . The use of the diffuse functions has been proved to be extremely important, since the geometry optimizations with nonaugmented basis functions resulted in large errors for the  $F^-H_b$  equilibrium distance.

The FPA study for the dissociation energy of  $F^-CH_4$  resulted in  $D_e$  and  $D_0$  values of  $2398 \pm 12$  and  $2280 \pm 20\text{ cm}^{-1}$ , respectively. The electron correlation has an extremely large, 39%, contribution to the  $D_e$  value. The effects of special relativity and the breakdown of the BO approximation have been found negligibly small. The  $D_e$  and  $D_0$  values have much better accuracy and lower uncertainty than the previous experimental and theoretical results; thus, we recommend to use these computed dissociation energies as benchmark values in the future.

The first 12-dimensional variational vibrational calculations have been performed for the  $F^-CH_4$  anion complex utilizing the newly developed global potential energy and dipole moment surfaces (PES and DMS, respectively). The PES of  $F^-CH_4$  has a correct dissociation behavior to the  $CH_4 + F^-$  channel, and this has been demonstrated by performing variational vibrational calculations for the  $CH_4$  molecule using the global PES of  $F^-CH_4$ . The vibrational spectrum for the  $F^-CH_4$  anion has been determined in the  $0-3000\text{ cm}^{-1}$  range. Infrared spectra have been measured in the CH stretching region ( $2400-3000\text{ cm}^{-1}$ ), and the variationally computed results are in good agreement with the experimental levels. The measured CH stretching frequency corresponding to the H-bond is  $2535\text{ cm}^{-1}$ , which was seriously overestimated by harmonic vibrational analysis. The variationally computed value of this study is  $2519\text{ cm}^{-1}$ , which agrees well with the measured frequency. There is a low-lying fundamental level ( $201\text{ cm}^{-1}$ ) corresponding to the intermolecular stretching mode of  $F^-$  having a relatively large intensity, but measurements have not been reported in this region of the spectrum.

**Acknowledgment.** Discussions with Mr. Etienne Garand on  $F^-CH_4/F-CH_4$  are gratefully acknowledged. G.C. thanks Ms. Yimin Wang for her help with the Multimode calculations. G.C. acknowledges support from the National Science Foundation, CRIF: CRF CHE-0625237. B.J.B. thanks the ONR (N00014-05-1-0460) for financial support.

## References and Notes

- (1) Wild, D. A.; Loh, Z. M.; Bieske, E. J. *Int. J. Mass Spectrom.* **2002**, *220*, 273–280.
- (2) Loh, Z. M.; Wilson, R. L.; Wild, D. A.; Bieske, E. J.; Gordon, M. S. *Aust. J. Chem.* **2004**, *57*, 1157–1160.

- (3) Loh, Z. M.; Wilson, R. L.; Wild, D. A.; Bieske, E. J.; Lisy, J. M.; Njagic, B.; Gordon, M. S. *J. Phys. Chem. A* **2006**, *110*, 13736–13743.
- (4) Wild, D. A.; Loh, Z. M.; Wolyneec, P. P.; Weiser, P. S.; Bieske, E. J. *Chem. Phys. Lett.* **2000**, *332*, 531–537.
- (5) Weiser, P. S.; Wild, D. A.; Wolyneec, P. P.; Bieske, E. J. *J. Phys. Chem. A* **2000**, *104*, 2562–2566.
- (6) Ayotte, P.; Kelley, J. A.; Nielsen, S. B.; Johnson, M. A. *Chem. Phys. Lett.* **2000**, *316*, 455–459.
- (7) Ayotte, P.; Nielsen, S. B.; Weddle, G. H.; Johnson, M. A.; Xantheas, S. S. *J. Phys. Chem. A* **1999**, *103*, 10665–10669.
- (8) Kawaguchi, K.; Hirota, E. *J. Chem. Phys.* **1986**, *84*, 2953–2960.
- (9) Neumark, D. M. University of California, Berkeley, CA. Personal communication, 2007.
- (10) Allen, W. D.; East, A. L. L.; Császár, A. G. In *Structures and Conformations of Non-Rigid Molecules*; Laane, J., Dakkouri, M., van der Veken, B., Oberhammer, H. Eds.; Kluwer: Dordrecht, The Netherlands, 1993; p 343.
- (11) Császár, A. G.; Allen, W. D.; Schaefer, H. F. *J. Chem. Phys.* **1998**, *108*, 9751–9764.
- (12) Dunning, T. H. *J. Chem. Phys.* **1989**, *90*, 1007–1023.
- (13) Hehre, W. J.; Radom, L.; Schleyer, P. v. R.; Pople, J. A. *Molecular Orbital Theory*; Wiley: New York, 1986.
- (14) Möller, C.; Plesset, M. S. *Phys. Rev.* **1934**, *46*, 618–622.
- (15) Čížek, J. *J. Chem. Phys.* **1966**, *45*, 4256–4266.
- (16) Raghavachari, K.; Trucks, G. W.; Pople, J. A.; Head-Gordon, M. *Chem. Phys. Lett.* **1989**, *157*, 479–483.
- (17) Kállay, M.; Gauss, J. *J. Chem. Phys.* **2005**, *123*, 214105.
- (18) MOLPRO, version 2006 1; a package of ab initio programs, written by Werner, H.-J.; Knowles, P. J.; Lindh, R.; Manby, F. R.; Schütz, M.; Celani, P.; Korona, T.; Rauhut, G.; Amos, R. D.; Bernhardsson, A.; Berning, A.; Cooper, D. L.; Deegan, M. J. O.; Dobbyn, A. J.; Eckert, F.; Hampel, C.; Hetzer, G.; Lloyd, A. W.; McNicholas, S. J.; Meyer, W.; Mura, M. E.; Nicklass, A.; Palmieri, P.; Pitzer, R.; Schumann, U.; Stoll, H.; Stone, A. J.; Tarroni, R.; Thorsteinsson T. See <http://www.molpro.net>.
- (19) MRCC, a string-based quantum chemical program suite written by Kállay, M. For the latest version, see <http://mrcc.hu>.
- (20) Kállay, M.; Surján, P. R. *J. Chem. Phys.* **2001**, *115*, 2945–2954.
- (21) Handy, N. C.; Yamaguchi, Y.; Schaefer, H. F. *J. Chem. Phys.* **1986**, *84*, 4481–4484.
- (22) The Mainz–Austin–Budapest version of ACES II Stanton, J. F.; Gauss, J.; Watts, J. D.; Szalay, P. G.; Bartlett, R. J. with contributions from Auer, A. A.; Bernholdt, D. B.; Christiansen, O.; Harding, M. E.; Heckert, M.; Heun, O.; Huber, C.; Jonsson, D.; Jusélius, J.; Lauderdale, W. J.; Metzroth, T.; Michauk, C.; O'Neill, D. P.; Price, D. R.; Ruud, K.; Schifmann, F.; Varner, M. E.; Vázquez, J. and the integral packages MOLUCULE Almlöf, J.; Taylor, P. R. *PROPS* Taylor, P. R., and *ABACUS* Helgaker, T.; Jensen, H. J. Aa.; Jørgensen, P.; Olsen, J.
- (23) Douglas, M.; Kroll, N. M. *Ann. Phys.* **1974**, *82*, 89–155.
- (24) Carter, S.; Bowman, J. M.; Handy, N. C. *Theor. Chem. Acc.* **1998**, *100*, 191–198.
- (25) Bowman, J. M.; Carter, S.; Huang, X. *Int. Rev. Phys. Chem.* **2003**, *22*, 533–549.
- (26) Watson, J. K. G. *Mol. Phys.* **1968**, *15*, 479–490.
- (27) Jung, J. O.; Gerber, R. B. *J. Chem. Phys.* **1996**, *105*, 10332–10348.
- (28) Carter, S.; Culik, S. J.; Bowman, J. M. *J. Chem. Phys.* **1997**, *107*, 10458–10469.
- (29) Wu, J.; Huang, X.; Carter, S.; Bowman, J. M. *Chem. Phys. Lett.* **2006**, *426*, 285–289.
- (30) Novoa, J. J.; Whangbo, M.-H.; Williams, J. M. *Chem. Phys. Lett.* **1991**, *180*, 241–248.
- (31) Heckert, M.; Kállay, M.; Tew, D. P.; Klopper, W.; Gauss, J. *J. Chem. Phys.* **2006**, *125*, 044108.
- (32) Hiraoka, K.; Mizuno, T.; Iino, T.; Eguchi, D.; Yamabe, S. *J. Phys. Chem. A* **2001**, *105*, 4887–4893.
- (33) Karton, A.; Martin, J. M. L. *Theor. Chem. Acc.* **2006**, *115*, 330–333.
- (34) Helgaker, T.; Klopper, W.; Koch, H.; Noga, J. *J. Chem. Phys.* **1997**, *106*, 9639–9646.
- (35) Huang, X.; Braams, B. J.; Bowman, J. M. *J. Chem. Phys.* **2005**, *122*, 044308.
- (36) Wang, Y.; Carter, S.; Braams, B. J.; Bowman, J. M. *J. Chem. Phys.* **2008**, *128*, 071101.
- (37) Wang, X. G.; Carrington, T. *J. Chem. Phys.* **2003**, *119*, 101–117.
- (38) Oyanagi, C.; Yagi, K.; Taketsugu, T.; Hirao, K. *J. Chem. Phys.* **2006**, *124*, 064311.
- (39) Mátyus, E.; Czakó, G.; Sutcliffe, B. T.; Császár, A. G. *J. Chem. Phys.* **2007**, *127*, 084102.
- (40) Schwenke, D. W.; Partridge, H. *Spectrochim. Acta, Part A* **2001**, *57*, 887–895.
- (41) Gray, D. L.; Robiette, A. G. *Mol. Phys.* **1979**, *37*, 1901–1920.